NANO LETTERS

2007
Vol. 7, No. 4
1044−1049

Identification of Quantum Dot Bioconjugates and Cellular Protein Co-localization by Hybrid Gel Blotting

Hong Yan Liu and Tania Q. Vu*

Department of Biomedical Engineering, Oregon Health & Science University, 3303 SW Bond Avenue, 13B, Portland, Oregon 97239

Received January 30, 2007; Revised Manuscript Received February 12, 2007

ABSTRACT

New approaches are needed to address the interaction of nanoparticles and cellular proteins at the molecular level. We present a modification of PAGE co-immunoprecipitation, QD-based PA-AGE electrophoresis blotting, and apply this to identify quantum dot (QD) bioconjugate–cellular protein association. This method provides the capability to isolate and evaluate the action of QD bioconjugate–protein complexes in intact cells and to correlate these identified interactions with their location in cells.

A goal of nanomedicine is to design multifunctional nanoscale platforms that can function to track and exert specific biological actions in cells. Quantum dots (QDs) show great promise as cellular effectors and reporters due to their unique combination of physiochemical and optical properties. QDs possess high surface-to-volume ratios and their sizes can be well-controlled, making them good candidates for interfacing with biological systems.[1−7] Moreover, QD fluorescence is intrinsic, bright, and prolonged, endowing QDs with "built-in" imaging functionality that exceeds the sensitivity and high-resolution capability of organic dyes and proteins.[1−4,8] Currently, a growing variety of bioconjugation techniques have been demonstrated to couple active proteins to QD surfaces with good success.[6,9−11] In addition, QDs have served as effective imaging agents for monitoring the movement of discrete biomolecules in cells.[12−16] Less clear is the identification of specific interactions of QD bioconjugates with cell surface and intracellular proteins. Initial studies show that QDs coated with ligands and targeting peptides can complex with cognate membrane receptors, cytoskeletal proteins, as well as associate with specifically designated nuclear and mitochondrial compartments.[13,16−23] However, QDs introduced into cells via various techniques such as endocytosis, microinjection, transfection, and other means, may associate with different cellular proteins over time inside cells, and molecular-based tools are needed to study QD bioconjugate−protein interactions at the molecular level.

Fluorescence co-localization has been commonly employed to assay QD−protein associations. With this technique, QD bioconjugates can be co-labeled with fluorescent antibodies to a protein that is presumed to interact with the QD bioconjugate. A significant limitation of fluorescence co-localization however, is that a protein species and QD bioconjugate may reside in close apposition but may not interact. Polyacrylamide gel electrophoresis (PAGE) based co-immunoprecipitation is an alternative and powerful approach that can be used to isolate specific protein species from cells and to their identify protein properties, such as phosphorylation state, or association with other cellular proteins, but QD bioconjugates either cannot enter polyacrylamide (PA) gels or be fractionalized by PAGE. While electrophoretic analysis has been used to successfully confirm the conjugation of biomolecules to QDs and gold nanoparticles,[9,24−28] these past methods have relied on agarose (AGE) gels and thus suffer from some limitations. AGE gels have large pore sizes and typically possess lower resolution separation capability than PAGE. While suitable for isolating higher weight molecular species, AGE gels lie at the limit of well-resolving finer QD size differences. In addition, AGE electrophoretic separation is based on charge density/size properties, and the inability to distinguish between these two factors can be confounding analytical limitation. Most importantly, AGE is not amenable to efficient electroblotting, thus making co-localization using Western blotting impractical.

Here, we describe a QD-based electrophoretic method that can be used to probe the integrity and activity of QD bioconjugates obtained from cells. Using a hybrid composition of polyacrylamide−agarose (PA-AGE), we show that cell-internalized QD bioconjugates can be visualized in situ as discrete QD bioconjugate−protein complexes and ex-

* Corresponding author. E-mail: tvu@bme.ogi.edu. Telephone: 503-418-9313.

10.1021/nl070239e CCC: $37.00
Published on Web 03/03/2007

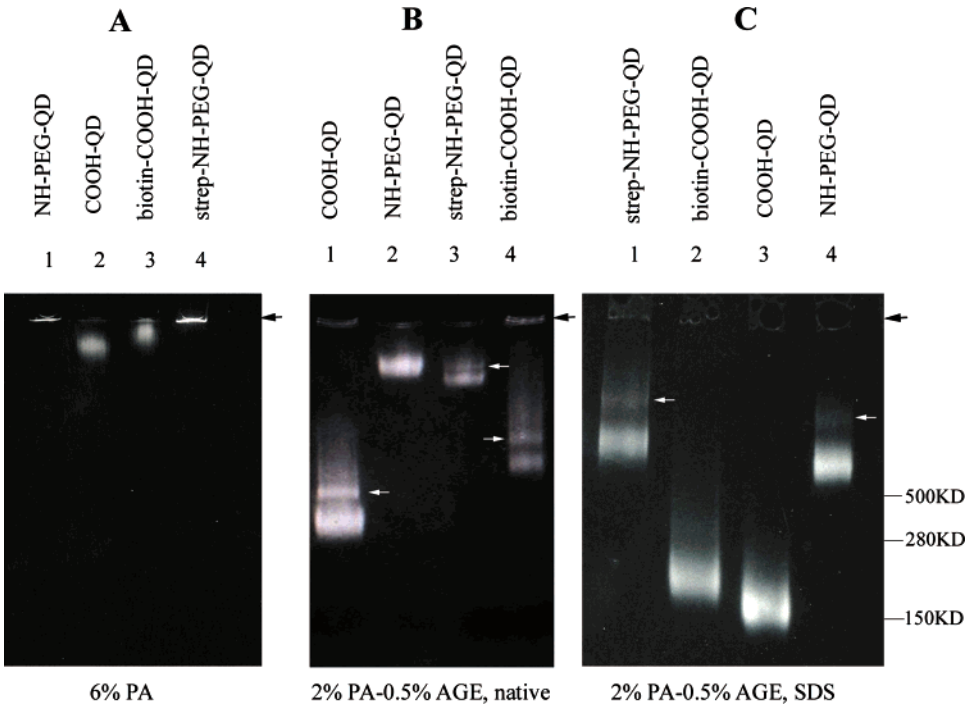

Figure 1. Well-resolved separation of quantum dots using hybrid PA-AGE gels. (A) Conventional native 6% PA gels severely retard QD entry and migration into gels for four types of QDs of different size and charge. (B) Hybrid 2%PA-0.5%AGE gels under native conditions (TBE, pH 8.3) separate QDs into tight bands. COOH-QDs and biotin-COOH-QDs are smaller and carry a greater negative charge density compared to streptavidin-NH-PEG-QDs and NH-PEG-QDs and migrate more quickly through the gel matrix. Further separation of QDs into subspecies (white arrows) highlights the separation capability of PA-AGE gels. (C) Under SDS, larger and less negatively charged NH-PEG-QDs and streptavidin-NH-PEG-QDs migrate more quickly through gels than under native conditions. Good separation resolution is evident as subspecies can be resolved (white arrows). Biotin-QDs and COOH-QDs are also well separated but migrate too quickly under these same conditions (100 V, 60 min) to resolve subspecies. Molecular weight markers show that PA-AGE gels can separate a wide range of apparent QD migration rates. Black arrows show loading position.

tracted from cells as discrete QD bioconjugate−protein complexes. Moreover, QD bioconjugate−protein complexes can be isolated by QD-based PA-AGE electrophoresis and blotted onto membranes for postanalysis of protein−protein interactions. QD-based PA-AGE electrophoresis blotting is an improved technique over conventional immunoprecipitation because time-consuming and extensive immunoprecipitation steps involving protein A/G-sepharose beads are eliminated. Most importantly, PA-AGE QD electrophoresis provides a sensitive means to isolate and evaluate the action of QD−protein complexes in intact cells.

Figure 1A shows that QD bioconjugates do not enter and separate well in standard 6% PA gels. In contrast, we find that a hybrid gels composed of 0.5−2.5% PA and 0.5−1.0% AGE are sturdy and easy to handle (PA-AGE gels) and serve to well-fractionate QD bioconjugates. Figure 1B,C demonstrates the separation capability of a 2% PA-0.5% AGE gel in native and SDS conditions using four different types of commercial QDs that vary in size and charge: (1) unconjugated COOH-655QDs, (2) COOH-655QDs conjugated with biotin, a vitamin with MW 244 and pI ∼ 3, (3) unconjugated NH-PEG-655QDs, and (4) NH-PEG-655QDs conjugated with streptavidin, a protein with MW 75 kD and pI ∼ 5−6. Figure 1B shows that all four types of QDs migrate and are well-fractionated in PA-AGE gels under native conditions. QDs are concentrated as tight bands of fluorescence with lack of significant smearing. Moreover, PA-AGE gels are capable of resolving subspecies of QD, as indicated by the presence of multiple gel bands (Figure 1, white arrows), which may reflect not only varying degrees of QD biofunctionalization, as in the case of biotin−QDs and streptavidin QDs, but also may reflect varying amounts ampiphilic polymer coating, as in the case of unconjugated COOH-QDs. Figure 1C shows that these QD bioconjugates can be treated with SDS. An advantage of these conditions is that added negative charge allows the heavier NH-PEG-QDs and streptavidin-NH-PEG-QDs to migrate faster compared to native conditions, allowing for better resolution of subspecies of QDs. Another advantage of SDS treatment is that the QD apparent migration rate in relation to protein markers can be approximated. Figure 1C shows that PA-AGE gels can separate a wide range of QD migration rates as measured in comparison to the migration of protein molecular weight markers (150 kD to >500 kD). We found that PA-AGE gels can separate proteins as small as 25 kD (the smallest molecular weight marker we tested). This indicates that the resolution limit of PA-AGE gels approaches that of PAGE.

To determine if QD PA-AGE can be used to visualize, isolate, and identify protein−protein interactions, we used this technique to investigate the association of ligand nerve growth factor (NGF)[16,28] with its cognate tyrosine kinase receptor, the trkA receptor.[29−31] NGF binds to trkA and is endocytosed into cells as a ligand−receptor complex.[32−35] We have shown in past work that QDs conjugated with nerve

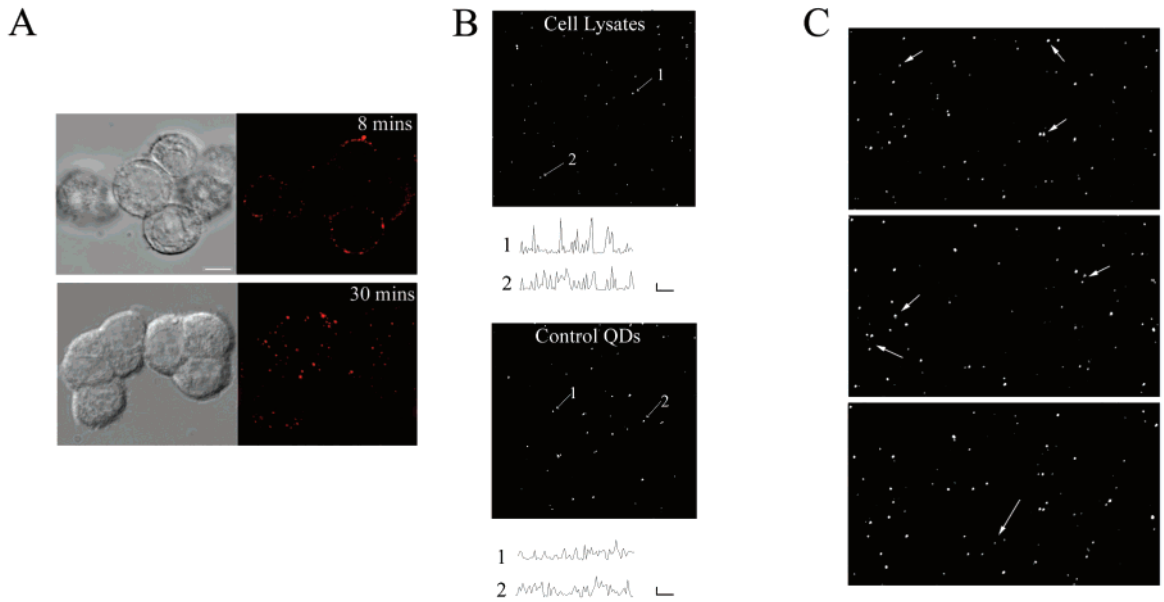

Figure 2. NGF-QDs provide subcellular localization of trkA receptors in cells and can be retrieved as discrete complexes from cellular lysates. (A) Live PC12 cells treated with NGF-QDs for 8 min exhibit discrete NGF-QDs that have bound to trkA receptor puncta on the cell membrane surface. After 30 min, discrete NGF-QDs are internalized into the cellular cytosol. Dark regions inside cells are nuclei. Scale bar: 5 μm. (B) Fluorescence microscope image of NGF-QDs from cellular lysates that have been cleared from PC12 cells treated with NGF-QDs for 30 min. Image shows that NGF-QDs exhibit fluorescence blinking behavior similar to that for the positive control (COOH-QDs alone), suggesting that NGF-QDs remain discrete and do not aggregate after cellular lysis. Scale bar: *x*-axis is 2.5 s, *y*-axis is 10 pixel intensity values. (C) A sequence of video stills showing that NGF-QDs retrieved from cell lysates of PC12 cells treated with NGF-QDs (30 min) are discrete and blinking. White arrows point to examples of discrete NGF-QDs that blink and are not present in all three successive stills.

growth factor (NGF) bind specifically to trkA receptors, induce trkA downstream signaling, and are internalized into cell bodies.[16,28] Conventional Western blots of lysates obtained from cells treated with NGF-QDs show that trkA is detectable and that NGF-QDs stimulate a profound increase in trkAs compared to baseline trkA of cells treated with null streptavidin QDs (Supporting Information). We treated PC12 cells with NGF-QDs and then determined if: (1) NGF-QDs could be retrieved and separated from a mixture of cellular lysate, and (2) if NGF-QDs were co-localized with an anti-trkA receptor antibody, indicating trkA−NGF-QD ligation.

Figure 2A shows that NGF-QDs can be used to identify the subcellular location of trkAs in live PC12 cells. Cells treated with NGF-QDs for 8 min exhibit discrete NGF-QDs that have bound to trkA receptor puncta on the cell membrane surface. As shown in our past studies, NGF-QDs are endocytosed into the cellular cytosol after 30 min, and a majority of QDs appear as discrete fluorescent particles inside cells.[16] When cells containing endocytosed NGF-QDs are lysed, we find that monodispersed QDs can be retrieved from cell lysates. Figure 2B shows a fluorescence microscope image of a cellular lysate from a cell treated with NGF-QDs that has been deposited onto a coverslip (1 μL). Cellular lysates contain discrete points of fluorescence. We consistently observe QDs, in the entire field of view, exhibiting fluorescence fluctuations or "blinking". This indicates that retrieved NGF-QD complexes consist of discrete QDs (Figure 2B).[2,36,37] These fluorescent intensity profiles are characteristic of NGF-QDs that are composed of individual or a few QDs.[16] Freely soluble COOH-QDs that are deposited directly onto coverslips serve as a positive control (Figure 2B), and as expected, exhibit blinking behavior similar to NGF-QDs cleared from cellular lysates. Figure 2C is a sequence of three video stills that shows NGF-QDs that have been retrieved from cells that have internalized QDs (NGF-QD treatment for 30 min) blink. White arrows point to examples of discrete NGF-QD fluorescence that is not present in all three successive stills. These data indicate that cell-endocytosed QDs can be successfully retrieved from cell lysates without aggregation for postanalysis.

PA-AGE electrophoresis and blotting can be performed to confirm the association of trkA to NGF-QDs in cells. Figure 3A shows that cell lysates containing NGF-QD complexes can be separated using native PA-AGE electrophoresis. NGF-QD treated cellular lysates are loaded at two different concentrations (lane 1: 40 μg; lane 3: 80 μg) and show clear fractionation in PA-AGE gels as well as differences in fluorescence density, which reflect the quantity of QDs at these two different concentrations (Figure 3A). As a control, soluble NGF-QDs that have not been exposed to cells have been loaded at two concentrations (lane 2: 1 μL, 10 nM NGF-QDs; lane 4: 2 μL, 10 nM NGF-QDs). The mobility of lysates from NGF-QD treated cells is slower than that for freely soluble NGF-QDs, suggesting that higher-molecular-weight trkA−NGF-QD complexes may have formed. PA-AGE gels can be faithfully transferred to membranes for further analysis, as shown by the fluorescence images taken with a color camera of electroblotted PVDF membrane replicas (Figure 3A).

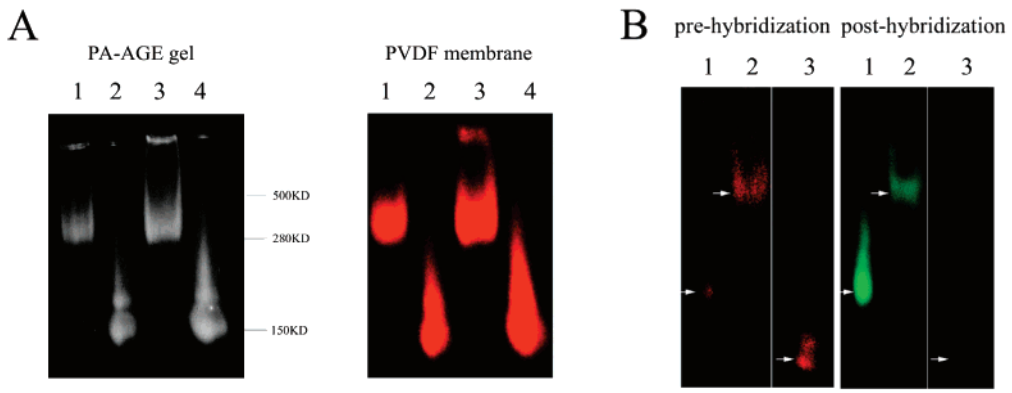

Figure 3. QD-based PA-AGE western blots for probing protein−protein interactions. (A) Left image shows PA-AGE separation of cellular lysates containing NGF-QDs from NGF-QD treated cells (30 min) for two concentrations of cell lysates (lane 1: 40 μg, lane 3: 80 μg). Cellular lysates containing NGF-QDs exhibit slower mobility compared to free NGF-QDs (lane 2: 1 μL; lane 4: 2 μL of 10 nM NGF-QDs), suggesting that cell exposed NGF-QDs have complexes with trkAs. Right-hand image is a fluorescence color camera image of electroblotted PVDF membranes indicating faithful transfer of NGF-QDs from gels to membranes. (B) Western blots show NGF-QDs obtained from cellular lysates are complexed to trkA receptors. Left hand image, lane 2, is the red channel of a color image taken from PA-AGE fractionated cellular lysates from cells exposed to NGF-QDs (30 min). Right-hand image, lane 2, is the green channel of a color image of the same PVDF membrane after hybridization with biotinylated anti-trkA, followed by streptavidin-525 QDs. NGF-QD cell lysates which hybridize in the same location and pattern with anti-trkA−biotin-streptavadin-525 QDs, indicating that NGF-QDs have bound to trkAs. Lane 1 contains free biotin-QDs (2 μL, 5 nM) and serves as a positive control, demonstrating that biotin-QD hybridizes with streptavidin-525 QDs, and as expected, migrate more quickly than NGF-QD cellular lysates (lane 2). Lane 3 contains free NGF-QDs (2 μL, 20 nM) and is a negative control showing lack of hybridization with either biotinylated anti-trkA or streptavidin-525 QDs.

Hybridization of NGF-QD blotted membranes allows identification of trkA−NGF-QD complexes. Figure 3B shows a red fluorescence image (red channel) of a PVDF membrane containing NGF-QDs that have been isolated from the lysate of cells treated with NGF-QDs (lane 2). The green fluorescence image (green channel) is this same blot after hybridization with a probe consisting of biotinylated anti-trkA followed by streptavidin-525 QDs. The correspondence both in shape and location of red (NGF-QDs) and green (biotinylated anti-trkA−streptavidin-525 QD) channels show that trkA−NGF-QD complexes have formed inside cells. Red biotin-QDs serve as a positive control and show hybridization with green streptavidin QDs (Figure 3B, lane 1). Moreover, freely soluble NGF-QDs serve as a negative control and do not hybridize when exposed to biotinylated anti-trkA and streptavidin QDs (Figure 3B, lane 3), demonstrating that binding of anti-trkA antibody to NGF-QD cell lysates is specific (Figure 3B, lane 2). These data demonstrate that QD bioconjugate−protein interactions may be analyzed on Western blots obtained from QD-based PA-AGE gels.

The use of PA-AGE hybrid gels allows separation of QDs with the improved resolution under both native and SDS conditions. We find that QDs that are functionalized with bioconjugates of varying size and charge are isolated and well-resolved, as shown by separation of QDs into subspecies. We have focused on isolating smaller-sized QDs that bear only polymeric coatings and QDs that are conjugated to low-molecular-weight proteins (rather than nucleic acids or large proteins) because these have been challenging to resolve. Because hybrid gels have been used to fractionate high-molecular-weight proteins such as immunoglobulins (IgM = 900 kDa) and nucleic acids,[38] it is expected that PA-AGE gels could be used to analyze QD bioconjugates over a wider size range. We find that QD bioconjugates exposed to cells can be retrieved as discrete QDs and efficiently transferred to membranes for Western blot post-analysis.

QD-based PA-AGE electrophoresis blotting is a procedure that may be useful for protein analysis and nanotechnology in several respects: (1) as a method for identifying specific QD−protein interactions in cells, (2) as a method for correlating QD targets with their spatial location in cells, (3) as a means to study the size and composition of QD bioconjugate probes, and finally, (4) as an improvement over traditional bead-based immunoprecipitation methods for directly isolating and visualizing proteins from complex mixtures.

Of particular note in the developing field of bionanotechnology is the need for molecular techniques to study the interactions of nanostructures with cellular proteins and to confirm that nanoparticle bioconjugates bind to their intended cellular targets. In addition to QDs, a variety of nanoparticle bioconjugates are in the pipeline for cellular delivery and targeting. We find that the composition of PA-AGE gels can be adjusted to separate and resolve QD bioconjugates that are complexed with cellular proteins. With appropriate modification, we expect that PA-AGE gel electrophoresis blotting will be suitable for confirming the specific binding of many different types of nanoparticle bioconjugates.

QD-based PA-AGE electrophoresis blotting, combined with the exceedingly bright and photostable luminescence properties of QDs, should provide investigators with a new rapid method for studying the interactions between QDs and proteins both in vitro and in situ.

Experimental Section. *PA-AGE Gel Preparation and Electrophoresis.* Gels composed of a mixture of acrylamide−agarose (2% PA-0.5% AGE) were prepared for QD-based PA-AGE electrophoresis blotting. AGE (1%) solution was

made by dissolving agarose (BioRad) in distilled water, boiling to melt, and cooled to 55 °C. PA (4%) gel was made with 30% acrylamide stock (29:1, acrylamide:bis) in 2× TBE buffer (pH = 8.3) and then put in 55 °C water bath for 10 min. Equal volumes of 1% AGE and 4% PA were mixed together, and ammonium persulfate was added to 0.05% (w/v) final concentration and TEMED was added to 1:5000 (v/v) to the solution. Hybrid PA-AGE gels were quickly poured into vertical slab gel apparatus and electrophoresis performed at 90−150 V for 1−2 h. The running buffer was 0.5× TBE under native conditions or 0.1% SDS. Apparent weights of QDs were determined using molecular weight markers (Hi Mark, Invitrogen, and Precision Plus protein dual color standards, Bio-Rad).

In-Gel Separation of trkA Receptors from Cells. NGF-QDs were synthesized by conjugation of β-NGF (R&D Systems) to COOH-QDs (Invitrogen/Quantum Dot Corporation). Conjugation was performed by reaction of NGF and QD (2:1 molar ratio) in 1-ethyl-3-(3-dimethylaminopropoyl)-carbodiimide (EDAC, Sigma-Aldrich) in borate buffer (pH 7.4) at room temperature for 2 h. PC-12 cells (ATCC) were grown in collagen-coated T-25 flasks in RPMI-1640 supplemented with 10% horse serum and 5% fetal bovine serum at 37 °C. Upon reaching confluence, PC12 cells were stimulated with 20 nm NGF-QDs in serum-free at 37 °C for 30 min. PC12 cells were lysed with lysis buffer (PBS, 10% glycerol and 0.25% NP-40) supplemented with protease inhibitor cocktail (Sigma) and phosphatase inhibitors (2 mM sodium orthovanadate and 10 mM sodium fluoride). Insoluble materials were removed from the protein extract by centrifugation (13 000 rpm, 15 min). Protein concentration in the cell lysates was measured using the Bio-Rad Protein Assay. Cell lysates were mixed with loading buffer (40% (w/v) sucrose, 0.25% (w/v) bromophenol blue) and loaded on PA-AGE gels under native conditions. In-gel imaging of QDs was performed with a hand-held Polaroid camera under UV transillumination.

Identification of NGF−trkA Protein Interactions. To identify proteins and probe protein−protein interactions, cell lysates obtained from NGF-QD treated cells were separated by PA-AGE gel electrophoresis and transferred to PVDF by electrophoretic blotting. (Mini Trans Blot Cell, Bio-Rad) in 0.5× TBE with 20% methanol under 100 V for 2−3 h. Images of protein-QD blotted PVDF membrane replicas were captured with a handheld color digital camera under UV transillumination. To probe NGF−trkA interactions, PVDF membranes were blocked with 3% BSA and subsequently incubated with a biotinylated-polyclonal anti-trkA antibody (C-14, sc-11, Santa Cruz). This anti-trkA was directed against an intracellular peptide within the C-terminus of the trkA receptor. Anti-trkA was biotinylated by incubation with 500-fold excess of NHS-PEO_4-biotin (Pierce), followed by dialysis (Slide-A-lyzer, 7KD MWCO, Pierce) against PBS (pH 7.2) to remove unbound biotin. Biotinylated anti-trkA was added to the blotting buffer (1× TBS/0.1% Tween-20) at a final concentration of 4 μg/mL. Subsequently, membranes were washed (3 times for 10 min each with 1× TBS/0.1% Tween-20) and streptavidin-525 QDs (green) were added (1nM in blotting buffer) for 1 h at room temperature. After washing (3 times for 10 min each with 1× TBS/0.1% Tween-20), images of PVDF membranes were captured with a digital camera under UV transillumination. For analysis of dual-fluorescence emission, grayscale information from separate red and green channels of a single color image were obtained by Adobe Photoshop (version 8) and pseudocolored using red and green look-up tables in Image J (NIH).

Microscope Imaging. Images were acquired using a Zeiss Axiovert microscope equipped with 40× and 100× objectives, excitation and emission filters (Chroma), and a cooled monochrome CCD camera (Axiocam). Fluorescent and bright-field optical sections of cells containing QDs were imaged using an Apotome unit (Zeiss) attached to the microscope (*z*-section thickness of 0.4 μm). Contrast and brightness of images were processed using Photoshop (Adobe version 8). QD fluorescence blinking was measured by placing a small volume of NGF-QDs in cell lysates (1 μL of 15 mg/mL protein) or freely soluble COOH-QDs (1 μL, 0.01nM) onto a coverslip. Time lapse videos of QD fluorescence blinking was captured at a 40 ms exposure time for durations of 20 s. Areas of QD fluorescence (0.1−0.25 μm^2) were selected using the outline measurement tool (AxionVision 4.4, Zeiss), and the integrated intensity in each selected area was plotted as a function of time.

Acknowledgment. This work was supported by Oregon ETIC research funds to T.Q.V. We thank Dr. Margo Haygood and Dr. Owen McCarty for insightful comments.

Supporting Information Available: Conventional Western blots detect trkA upregulation in NGF-QD stimulated cells. This material is available free of charge via the Internet at http://pubs.acs.org.

References

(1) Michalet, X.; Pinaud, F. F.; Bentolila, L. A.; Tsay, J. M.; Doose, S.; Li, J. J.; Sundaresan, G.; Wu, A. M.; Gambhir, S. S.; Weiss, S. *Science* **2005**, *307*, 538−544.
(2) Chan, W. C.; Nie, S. *Science* **1998**, *281*, 2016−2018.
(3) Bruchez, M., Jr.; Moronne, M.; Gin, P.; Weiss, S.; Alivisatos, A. P. *Science* **1998**, *281*, 2013−2016.
(4) Alivisatos, A. P.; Gu, W.; Larabell, C. *Annu. Rev. Biomed. Eng.* **2005**, *7*, 55−76, 53 plates.
(5) Smith, A. M.; Ruan, G.; Rhyner, M. N.; Nie, S. *Ann. Biomed. Eng.* **2006**, *34*, 3−14. Epub 2006 Feb 2001.
(6) Medintz, I. L.; Uyeda, H. T.; Goldman, E. R.; Mattoussi, H. *Nat. Mater.* **2005**, *4*, 435−446.
(7) Niemeyer, C. M. *Angew. Chem., Int. Ed.* **2001**, *40*, 4128−4158.
(8) Grecco, H. E.; Lidke, K. A.; Heintzmann, R.; Lidke, D. S.; Spagnuolo, C.; Martinez, O. E.; Jares-Erijman, E. A.; Jovin, T. M. *Microsc. Res. Tech.* **2004**, *65*, 169−179.
(9) Pinaud, F.; King, D.; Moore, H. P.; Weiss, S. *J. Am. Chem. Soc.* **2004**, *126*, 6115−6123.
(10) Howarth, M.; Takao, K.; Hayashi, Y.; Ting, A. Y. *Proc. Natl. Acad. Sci. U.S.A.* **2005**, *102*, 7583−7588.
(11) Goldman, E. R.; Balighian, E. D.; Mattoussi, H.; Kuno, M. K.; Mauro, J. M.; Tran, P. T.; Anderson, G. P. *J. Am. Chem. Soc.* **2002**, *124*, 6378−6382.
(12) Lidke, D. S.; Nagy, P.; Heintzmann, R.; Arndt-Jovin, D. J.; Post, J. N.; Grecco, H. E.; Jares-Erijman, E. A.; Jovin, T. M. *Nat. Biotechnol.* **2004**, *22*, 198−203. Epub 2004 Jan 2004.
(13) Courty, S.; Luccardini, C.; Bellaiche, Y.; Cappello, G.; Dahan, M. *Nano Lett* **2006**, *6*, 1491−1495.
(14) Michalet, X.; Pinaud, F.; Lacoste, T. D.; Dahan, M.; Bruchez, M. P.; Alivisatos, A. P.; Weiss, S. *Single Molecules* **2001**, *2*, 261−276.

(15) Yano, H.; Ninan, I.; Zhang, H.; Milner, T. A.; Arancio, O.; Chao, M. V. *Nat. Neurosci.* **2006**, *9*, 1009−1018. Epub 2006 Jul 1002.
(16) Sundara Rajan, S.; Vu, T. Q. *Nano Lett* **2006**, *6*, 2049−2059.
(17) Rosenthal, S. J.; Tomlinson, I.; Adkins, E. M.; Schroeter, S.; Adams, S.; Swafford, L.; McBride, J.; Wang, Y.; DeFelice, L. J.; Blakely, R. D. *J. Am. Chem. Soc.* **2002**, *124*, 4586−4594.
(18) Young, S. H.; Rozengurt, E. *Am. J. Physiol. Cell Physiol.* **2006**, *290*, C728−732. Epub 2005 Oct 2019.
(19) Howarth, M.; Takao, K.; Hayashi, Y.; Ting, A. Y. *Proc. Natl. Acad. Sci. U.S.A.* **2005**, *102*, 7583−7588. Epub 2005 May 7516.
(20) Hoshino, A.; Fujioka, K.; Oku, T.; Nakamura, S.; Suga, M.; Yamaguchi, Y.; Suzuki, K.; Yasuhara, M.; Yamamoto, K. *Microbiol. Immunol.* **2004**, *48*, 985−994.
(21) Calabretta, M.; Jamison, J. A.; Falkner, J. C.; Liu, Y.; Yuhas, B. D.; Matthews, K. S.; Colvin, V. L. *Nano Lett.* **2005**, *5*, 963−967.
(22) Gussin, H. A.; Tomlinson, I. D.; Little, D. M.; Warnement, M. R.; Qian, H.; Rosenthal, S. J.; Pepperberg, D. R. *J. Am. Chem. Soc.* **2006**, *128*, 15701−15713.
(23) Chen, F.; Gerion, D. *Nano Lett.* **2004**, *4*, 1827−1832.
(24) Sandstrom, P.; Akerman, B. *Langmuir* **2004**, *20*, 4182−4186.
(25) Zanchet, D.; Micheel, C. M.; Parak, W. J.; Gerion, D.; Alivasatos, A. P. *Nano Lett.* **2001**, *1*, 32−35.
(26) Pons, T.; Uyeda, H. T.; Medintz, I. L.; Mattoussi, H. *J. Phys. Chem. B* **2006**, *110*, 20308−20316.
(27) Park, S.; Brown, K. A.; Hamad-Schifferli, K. *Nano Lett.* **2004**, *4*, 1925−1929.
(28) Vu, T. Q.; Maddipati, R.; Blute, T. A.; Nehilla, B. J.; Nusblat, L.; Desai, T. A. *Nano Lett.* **2005**, *5*, 603−607.
(29) Segal, R. A. *Annu. Rev. Neurosci.* **2003**, *26*, 299−330. Epub 2003 Feb 2018.
(30) Sofroniew M. V., H. C.; Mobley, W. C. *Annu. Rev. Neurosci.* **2001**, *24*, 1217−1281.
(31) Huang, E. J.; Reichardt, L. F. *Annu. Rev. Neurosci.* **2001**, *24*, 677−736.
(32) Grimes, M. L.; Zhou, J.; Beattie, E. C.; Yuen, E. C.; Hall, D. E.; Valletta, J. S.; Topp, K. S.; LaVail, J. H.; Bunnett, N. W.; Mobley, W. C. *J. Neurosci.* **1996**, *16*, 7950−7964.
(33) Sorkin, A.; Von Zastrow, M. *Nat. Rev. Mol. Cell Biol.* **2002**, *3*, 600−614.
(34) Zapf-Colby, A.; Olefsky, J. M. *Endocrinology* **1998**, *139*, 3232−3240.
(35) Howe, C. L.; Mobley, W. C. *Curr. Opin. Neurobiol.* **2005**, *15*, 40−48.
(36) Yao, J.; Larson, D. R.; Vishwasrao, H. D.; Zipfel, W. R.; Webb, W. W. *Proc. Natl. Acad. Sci. U.S.A.* **2005**, *102*, 14284−14289. Epub 12005 Sep 14216.
(37) Zhang, K.; Chang, H.; Fu, A.; Alivisatos, A. P.; Yang, H. *Nano Lett* **2006**, *6*, 843−847.
(38) Elkon, K. B.; Jankowski, P. W.; Chu, J. L. *Anal. Biochem.* **1984**, *140*, 208−213.

NL070239E